ADVANCED FUNCTIONAL MATERIALS

Supporting Information

for *Adv. Funct. Mater.,* DOI: 10.1002/adfm.201504076

Proton Transport in Electrospun Hybrid Organic–Inorganic Membranes: An Illuminating Paradox

*Leslie Dos Santos, Manuel Maréchal, Armel Guillermo, Sandrine Lyonnard, Simona Moldovan, Ovidiu Ersen, Ozlem Sel, Hubert Perrot, and Christel Laberty-Robert**

Supporting Information

Proton Transport in Hybrid Organic-Inorganic Membrane: An Illumitating Paradox

*L. Dos Santos, M. Maréchal, A. Guillermo, S. Lyonnard, S. Moldovan, O. Ersen, O; Sel, H. Perrot and Ch. Laberty–Robert**

Part I. Characterization of the membrane

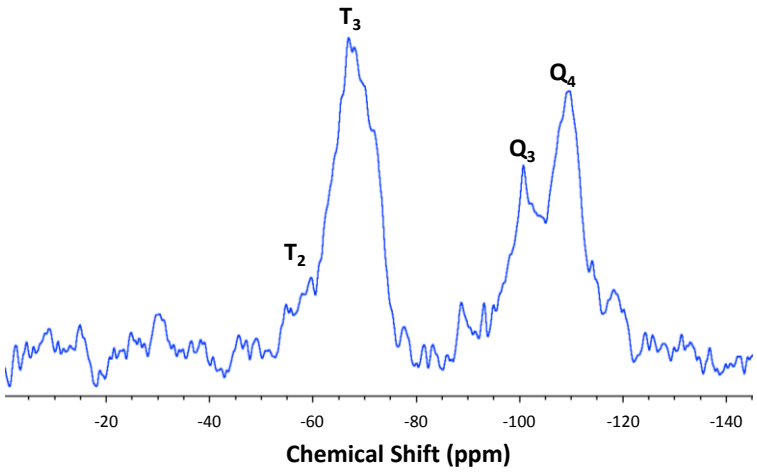

Figure SI 1. ^{29}Si NMR spectra of HM.

Part II. Electrochemical Impedance Spectroscopy (EIS) on Electrospun Hybrid Membranes

A bilayer architecture consisting of a mediator film/hybrid electrospun membrane is fabricated on the gold electrode (gold foil, 0.05 mm thickness, 99.95% purity (Goodfellow)) (**Figure SI 2**). The mediator film is composed of a heteropolyanion ((HPA)–$SiMo_{12}O_{40}^{4-}$) encapsulated in a polypyrrole conducting polymer matrix. HPA acts as a redox couple, electron and proton exchanger, while the polypyrrole conductive matrix serves as a support to

immobilize the HPA. The electrochemical reactions corresponding to the redox behavior of the HPA (**Figure SI 3**) are shown below:

$$SiMo^{VI}_{12}O_{40}^{4-} + 2\,H^{+} + 2\,e^{-} \leftrightarrows H_2SiMo^{VI}_{10}Mo^{V}_{2}O_{40}^{4-} \quad \text{(Reaction I)}$$

$$H_2SiMo^{VI}_{10}Mo^{V}_{2}O_{40}^{4-} + 2\,H^{+} + 2\,e^{-} \leftrightarrows H_4SiMo^{VI}_{8}Mo^{V}_{4}O_{40}^{4-} \quad \text{(Reaction II)}$$

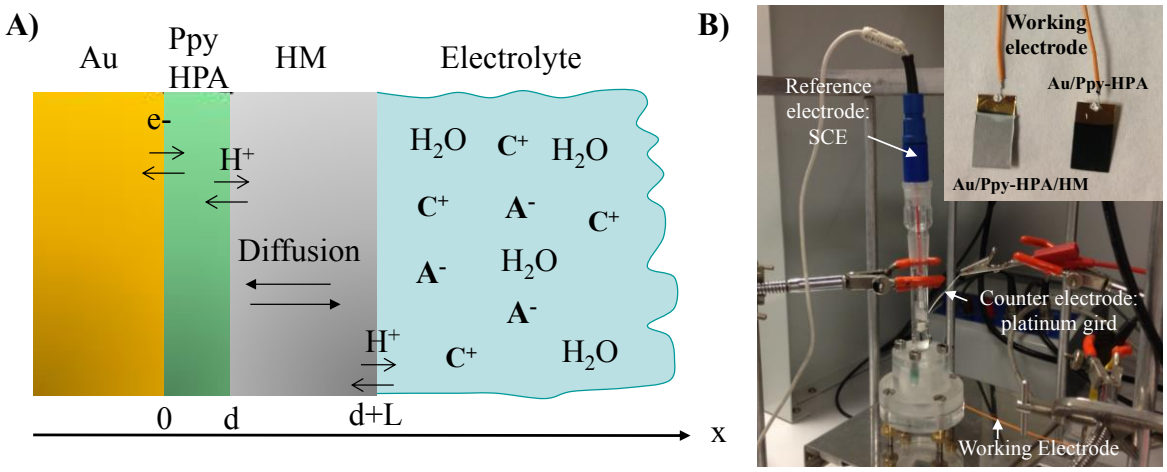

Figure SI 2. (a) Schematic representation of the interfaces in the bilayer electrode (Au/Ppy–HPA/HM) in contact with the electrolyte (C^{+}: cations, A^{-}: anions, H^{+}: proton) and **(b)** an image showing the experimental set-up for the 3–electrode system.

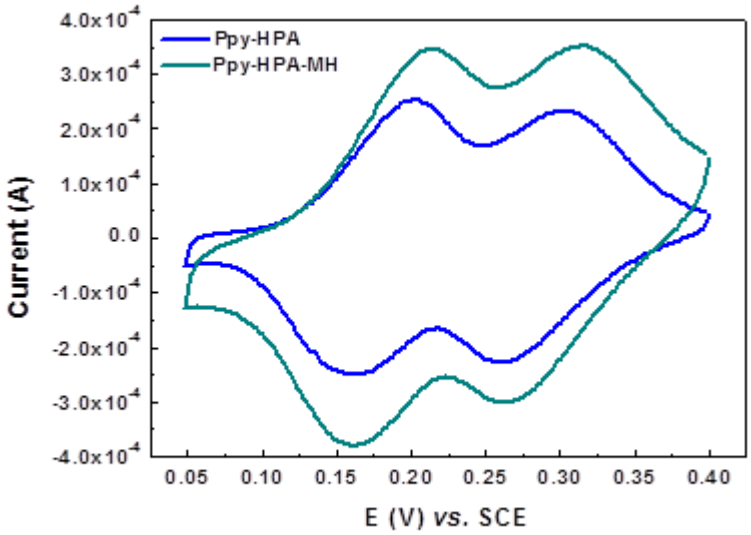

Figure SI 3. The cyclic voltammograms of PPy–HPA and PPy–HPA/HM bilayer electrode deposited on the gold substrates and measured in aqueous 0.5 M $HClO_4$.

The mediator film (HPA) is necessary to provide the H^+ transfer between the interfaces and therefore to study the proton transport inside the electrospun membrane which is only an ionic conductor (**Figure SI 2**). The illustration of the studied bilayer (**Figure SI 2a)** shows that the electronic transfer occurs at the gold electrode/mediator film interface. For a cathodic potential increase, the protons enter the HM from the solution which constitutes the HM/solution interface and subsequently diffuse in the membrane up to the PPy–HPA/HM interface, where they are inserted. The derivation of the final transfer function, electrochemical impedance ($\frac{\Delta E}{\Delta I}(\omega)$) for the theoretical model taking into account the transport phenomenon is detailed in reference [S1]. The key reactions are summarized below.

Part II A: Theoretical Model

At the PPy–HPA/HM interface (at x = d, **Figure SI2a**), protons, are inserted or expelled from the mediator film:

$$\langle\ \rangle_{HPA} + H^+_{HM} + e^- \underset{k_1}{\overset{k_2}{\rightleftharpoons}} \langle H\rangle_{HPA} \qquad \text{[Eq. S1]}$$

where H^+_{HM} is the proton diffusing in the electrospun HM, $\langle\ \rangle_{HPA}$ represents the available sites for ion insertion in the mediator film and $\langle H\rangle_{HPA}$ is the concentration of the protons inserted in the mediator film.

Then, the flux of protons, $J_{H^+}(d)$, entering the mediator film is equal to:

$$J_{H^+}(d) = k_2\left(c^{HPA}_{max} - c^{HPA}_{H^+}\right)c^{HM}_{H^+}(d) - k_1(c^{HPA}_{H^+} - c^{HPA}_{min}) \qquad \text{[Eq. S2]}$$

where $c^{HPA}_{H^+}$ is the proton concentration in the PPy−HPA film, $c^{HM}_{H^+}(d)$ is the concentration of the protons in the HM, close to the PPy−HPA/HM interface (x = d), c^{HPA}_{max} and c^{HPA}_{min} are the maximum and minimum concentrations of the protons in the PPy−HPA film, and $k_i = k_i^0 \exp(b_i E)$ are the classical Tafel kinetic rate constants.

Therefore, for a small potential perturbation, ΔE, the change of the proton flux, ΔJ_{H^+} at $x = d$, is equal to:

$$\Delta J_{H^+}(d) = G_{H^+}^{HPA/HM}\Delta E + K_{H^+}^{HPA/HM}\Delta c_{H^+}^{HPA} + M_{H^+}^{HPA/HM}\Delta c_{H^+}^{HM}(d)$$

[Eq. S3]

where

$K_{H^+}^{HPA/HM} = k_1 + k_2 c_{H^+}^{HM}(d)$
$G_{H^+}^{HPA/HM} = b_2 k_2 \left(c_{max}^{HPA} - c_{H^+}^{HPA}\right) c_{H^+}^{HM}(d) - b_1 k_1 \left(c_{H^+}^{HPA} - c_{min}^{HPA}\right)$
$M_{H^+}^{HPA/HM} = k_2 (c_{max}^{HPA} - c_{H^+}^{HPA})$

are the kinetic constants related to the transfer at the PPy-HPA/HM interface. The equation describing the faradic electrochemical impedance, $\frac{\Delta E}{\Delta I}(\omega)$ which takes into account the diffusion phenomenon ($j\omega\Delta C^{HPA/HM} = D\frac{\partial^2 \Delta C^{HPA/HM}}{\partial x^2}$) was given in Ref. **S1**, and it is equal to:

$$\frac{\Delta E}{\Delta I}(\omega) = \frac{1}{FG_{H^+}^{HPA/HM}}\left(1 - M_{H^+}^{HPA/HM}\frac{\tanh\left(-L\sqrt{\frac{j\omega}{D_{H^+}^{HM}}}\right)}{\sqrt{j\omega D_{H^+}^{HM}}}\right) - \frac{K_{H^+}^{HPA/HM}}{j\omega dFG_{H^+}^{HPA/HM}} \qquad \text{[Eq. S4]}$$

where L is the HM thickness and $D_{H^+}^{HM}$ is the diffusion coefficient of the protons in the HM. The equation S4 was used to fit of the experimental electrochemical impedance data in this study. In our basic approach, to simplify the analytical model, only diffusion is taken into account, the migration effect has been considered as a minor contribution. This can be justified by the fact that without a mediator film, which acts as a "proton pump", the electrochemical response is drastically different under the same experimental conditions.

Part II B: Detailed Experimental Conditions:

Electrochemical Synthesis of the PPy–HPA thin films. The mediator film is synthesized by encapsulating heteropolyanions ($SiMo_{12}O_{40}^{4-}$) in a polypyrrole film. The gold substrates were

cut into 1cm x 2cm dimension (gold foil, 0.05 mm thickness, 99.95% purity (Goodfellow)) and were cleaned by piranha solution (H_2O_2/H_2SO_4; 1v:3v) for 10 min. The films of PPy-HPA were synthesized by galvanostatic electrodeposition. To do this, 3.57 mL of α-$H_4SiMo_{12}O_{40}$ solution (Aldrich) was mixed with 25 ml of water (the α-$H_4SiMo_{12}O_{40}$ concentration is 2.10^{-2} M) and 16.6 µL of previously distilled pyrrole monomer was added to the solution. The film was obtained through a galvanostatic regime at a current value of 150 uA for 625 seconds. The reference electrode was a saturated calomel electrode (SCE), the counter electrode was a platinum grid. An equivalent film thickness of ~ 300 nm was estimated by scanning electron microscopy. Before the electrospun HM deposit, the mediator film was equilibrated by cyclic voltammetry in an aqueous solution of 0.5 M $HClO_4$. Twenty cycles were performed between 0.05V and 0.40V vs ECS with a scan rate of 20 mV s^{-1}.

Hybrid Membrane Deposition by Electrospinning. The hybrid membrane is then deposited on the modified substrate (PPy-HPA on gold) by "electrospinning" for 20 min at 0.1 mL/min and 26 kV. The characteristics of the solution used are as follows: 600 mg of PVDF-HFP (Solvay chemicals) is dissolved in 7mL of DMF (Sigma-Aldrich). Then two silica precursors: 361 mg of tetraethyl orthosilicate (TEOS) (Sigma-Aldrich), 2357 mg of 2-(4-chlorosulfonylphenyl)ethyltrichlorosilane) 50% in methylene chloride (CSPTc) (ABCR) and two additives: 340 mg of polyethylene glycol (Mn 285-315) (Sigma-Aldrich) and 312 mg of PVDF–2–hydroxy (Specific Polymers) are added. Inorganic weight percentage of the solution is 55%, and TEOS /CSPTc molar ratio is 1/2. The resulting solution is stirred for 3 h at 70° C before electrospinning. Finally, the membrane is dry at 70°C during 24 hours. The thickness of the electrospun hybrid membrane is ~ 36 microns.

Part III. NMR calibration of the molar ratio [H_2O]/[SO_3]:

The ^1H chemical shift of water inside Nafion membranes is known to be dependent on the amount of water molecules around the sulfonic acid groups localized at the ends of the side-chains.[S2] A fast exchange of hydrogens between the two species H_2O and $H_3O^+ \ldots SO_3^-$

results in a linear dependence of the water chemical shift vs λ^{-1}, λ being the molar ratio $[H_2O]/[SO_3H]$.[S3] The λ–dependence of the water chemical shift we measured for a Nafion membrane is depicted in **Figure SI 4**. Considering the hypothesis that the water chemical shift is only dependent on the number of water molecules per sulfonic group, the number λ characterizing the hydration level of sulfonated hybrid membranes was determined using this calibration curve.

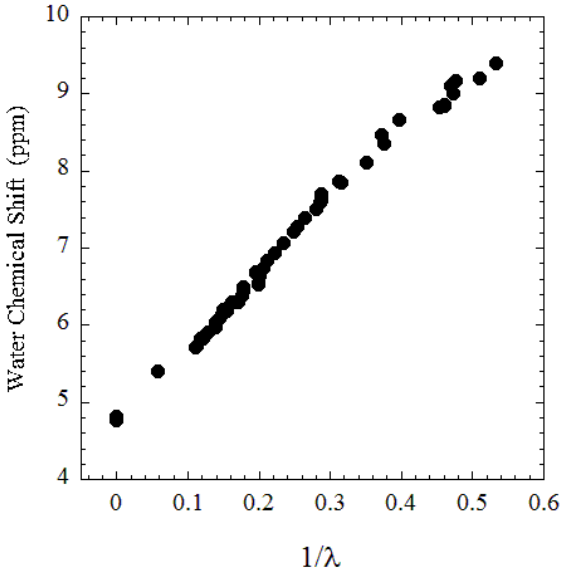

Figure SI.4. Calibration λ vs ^{1}H water chemical shift for a sulfonic acid membrane.

The calibration curve was established using a Nafion membrane (Ionic Exchange Capacity 0.91 meq/g, Equivalent Weight 1100 g/eq). In this experiment, λ was determined by using the integral of water resonance lines to measure the amount of water inside membranes; the calibration resonance line integral *vs* weight of water was assessed using samples with known amounts of water.

Part IV. QENS studies

Part IV A – Samples preparation, data acquisition and treatment.

Membranes prepared at fixed hydration (λ=1, 2.4 and 6.7) were enclosed in a 1 mm thick Aluminium flat container, that was sealed with indium wire to insure tightness. The sample

transmissions were checked to be higher than 95%, such that multiple scattering effects are negligible. The raw S(θ,t) data, where θ and t are the scattering angle and the time-of-flight, were transformed into S(Q,ω), where Q is the momentum transfer and ω is the energy transfer, using the usual ILL routines. The quasielastic spectra S(Q,ω) were then corrected from sample container and detector efficiency. A flat piece of vanadium was used to measure the experimental resolution function Re(ω). The spectra were adjusted to theoretical model functions in the ω-range [-0.5, 0.3 meV].

Part IV B – Data analysis using phenomenological models

Data acquired on the IN5 time–of–flight (TOF) spectrometer were first fitted using a single-Lorentzian component to account for the proton dynamics. The experimental S(Q,ω) were compared with the following theoretical S(Q,ω) function:

$$S(Q,\omega) = DW[A(Q)L(\omega) + P(Q) + B] \otimes Re(Q,\omega) \qquad \text{[Eq. S5]}$$

where DW is the Debye-Waller factor, L(ω) the quasielastic Lorentzian component of Half-Width at Half Maximum (HWHM) Γ, A(Q) the quasielastic structure factor, P(Q) the elastic contribution, B a flat background and Re(Q,ω) the instrumental resolution. P(Q) contains the coherent scattering component due to non-moving atoms (on the time-scale of the experiment, *i.e.* 0.1 – 50 ps), *i.e.* the host matrix. An example of fit is shown on **Fig. SI 5a** in the case of the most hydrated sample. Clearly, the data are not satisfactorily reproduced, as the single-Lorentzian approach leads to over (under) estimate the signal at low (high) energy transfer. There is a need for at least an additional Lorentzian component. Yet, it can be interestingly noticed that the mean HWHM is in the range [30-50 μeV] with a tendency to a low-Q plateau behavior, which is the usual signature of confined motions (**Figure SI 5b)**. In a second step, the data were therefore fitted using two Lorentzian components, labeled respectively large and narrow, according to the equation:

$$S(Q,\omega) = DW \times \left(A_{large}(Q)\frac{\Gamma_{large}(Q)^2}{\Gamma_{large}(Q)^2 + \omega^2} + A_{narrow}(Q)\frac{\Gamma_{narrow}(Q)^2}{(\Gamma_{narrow}(Q))^2 + \omega^2} + P(Q)\delta(\omega) \right) \otimes Res(\omega)$$

[Eq. S6]

The data can be much better approximated using the two-Lorentzian analysis over the Q-range, even if it has to be noticed that at low Q values the fits are difficult due to low intensities (especially for the "almost-dry" membrane due to very low amount of protons, λ=1). The large component shows a mildly dispersive HWHM (**Figure SI 6a**). The values are randomly scattered around a mean value of 0.35 meV at all hydrations, corresponding to a characteristic time of 1.9 ps, close to the value found in bulk water (e.g. 1.5 ps) for rotational motions. The second Lorentzian is roughly ten times narrower, in the range 10-40 μeV. It corresponds to molecular motions that are ten times slower than the previous ones. The HWHM of the narrow component exhibits a significant Q-dependence (**Figure SI 6b**) for hydrated samples, hence indicating a diffusive behavior on the timescale of typically few tens of picoseconds. Yet, the variations of the intensities were not showing physical variations that could be exploited using standard diffusion models. Consequently, it appeared that we had to consider the large component as a fixed-width Lorentzian to reduce the degree of freedoms of the fitting process and obtain more accurate information on the component of interest, e.g. the slow translational motions associated to the narrow part of the quasielastic wings. In addition, we proceeded to an analysis of the narrow quasi-elastic signal using the Gaussian model in order to extract quantitative parameters.

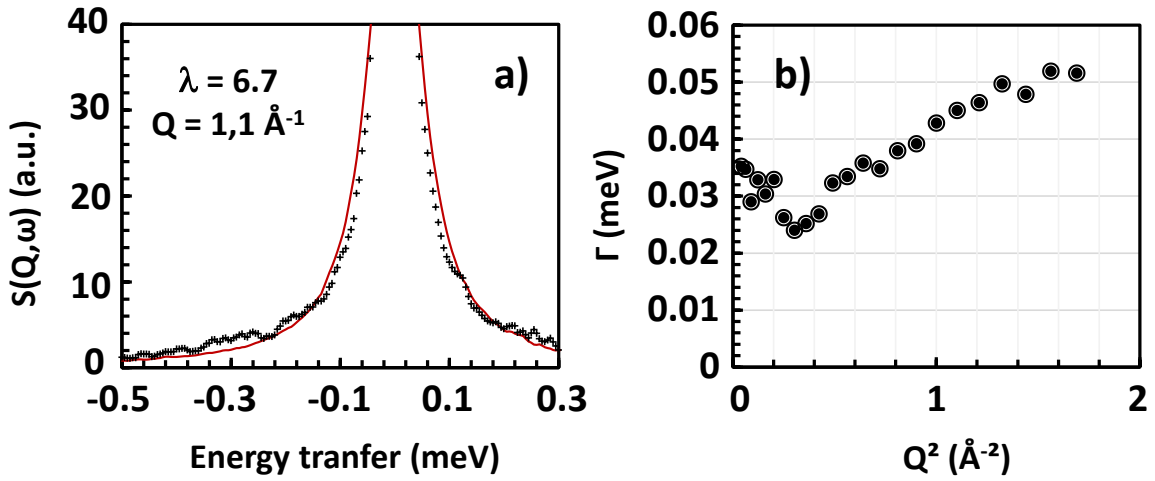

Figure SI 5. a) S(Q,ω) of the λ= 6.7 sample displayed at Q = 1.1 Å^{-1}. Dots are experimental points, the line represents the theoretical function calculated from Eq. 1.**b)** HWHM of the Lorentzian function vs Q².

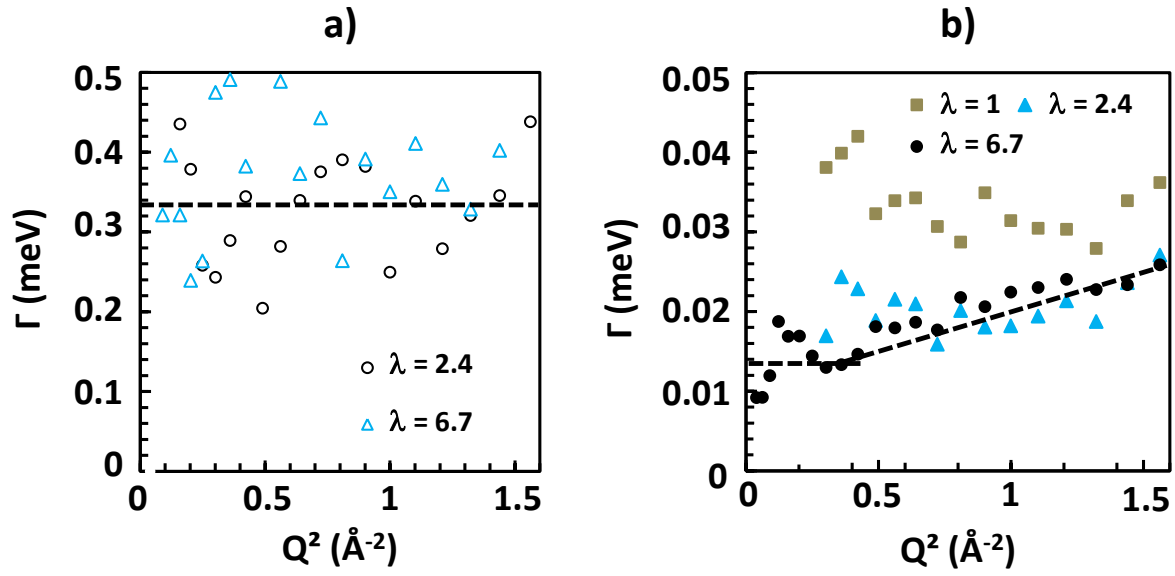

Figure SI 6. Q-dependence of the HWHM of the large **(a)** and narrow **(b)** Lorentzian components obtained by analyzing the hybrid membrane spectra with eq. 2..

Part IV C – Data analysis using the Gaussian model

The Gaussian model for localized translational motion is described in details in reference [S4]. The Gaussian S(Q,ω) is an infinite sum of Lorentzian curves modulated by structure factors :

$$S(Q,\omega) = e^{-Q^2\sigma^2}.\left(\delta_0 + \sum_{n=1}^{\infty} \frac{(Q^2\sigma^2)^n}{n!} \frac{n.\Gamma_0}{\omega^2+(n.\Gamma_0)^2}\right) \qquad \text{[Eq. S7]}$$

with σ the variance of the Gaussian distribution.

In the present case, we restricted the infinite sum to the first two terms, namely L_0 and L_1, which mostly contribute to the intensity in the available limited Q-range of our experiments. L_0 is a Lorentzian of width Γ_0, and Γ_1 has a width of $\Gamma_1=2\Gamma_0$ [4]. We adjusted the hybrid membranes data using these two components (Γ_0 is a free parameter) and adding a broad constant-width component L_2 to account for fast rotations. Γ_2 was fixed at 0.35 meV according to the previous two−Lorentzian analysis in **Figure SI 6**. On **Figure 5b** in the paper; the best overall fits (for λ= 6.7 membrane) are achieved with the total S(Q,ω) function including an elastic term and three Lorentzian functions L_0, L_1 and L_2 :

$$S(Q,\omega) = DW \times \left[f0(Q)\frac{\Gamma_0(Q)^2}{\Gamma_0(Q)^2 + \omega^2} + f1(Q)\frac{(2\Gamma_0(Q))^2}{(2\Gamma_0(Q))^2 + \omega^2} + f2(Q)\frac{\Gamma_2(Q)^2}{\Gamma_2(Q)^2 + \omega^2} + P(Q)\delta(\omega) \right] \otimes Res(\omega)$$

[Eq. S8]

The coefficients $f_i(Q)$ are the Gaussian structure factors, as described in reference. [S4] Γ_0 was found equal to 15 μeV for the three hybrid membranes. The data are well reproduced over the whole Q-range, thus supporting the choice of the Gaussian model. Moreover, the variations of the integrated intensities of the diffusive quasielastic responses L_0 and L_1 can be analysed using the Gaussian model structure factors $f_0(Q)$ and $f_1(Q)$ (**Figure SI 7**). The evolution of L_0 intensities for the three membranes are shown on **Figure SI 7a** to highlight the effect of water content on the local proton dynamics, e.g. increased intensities indicating the enhancement of mobile protons. Moreover, the maximum of the intensity of the quasielastic signal L_0 is related to the size of the confining water droplet, 2σ. It is shifted towards small Q values when the hydration level in the membrane increases, indicating the increased values of σ. We found 2σ equal to 1.2, 2 and 2.6 Å, for the membranes equilibrated at λ= 0, 2.4 and 6.7 respectively. **Figure SI 7b** shows how σ values are determined from fitting the quasi-elastic integrated intensities of L_0 and L_1 components using the Gaussian functions $f_0(Q)$ and $f_1(Q)$ modulated by the Debye-Waller factor (which produces the large-Q decay).

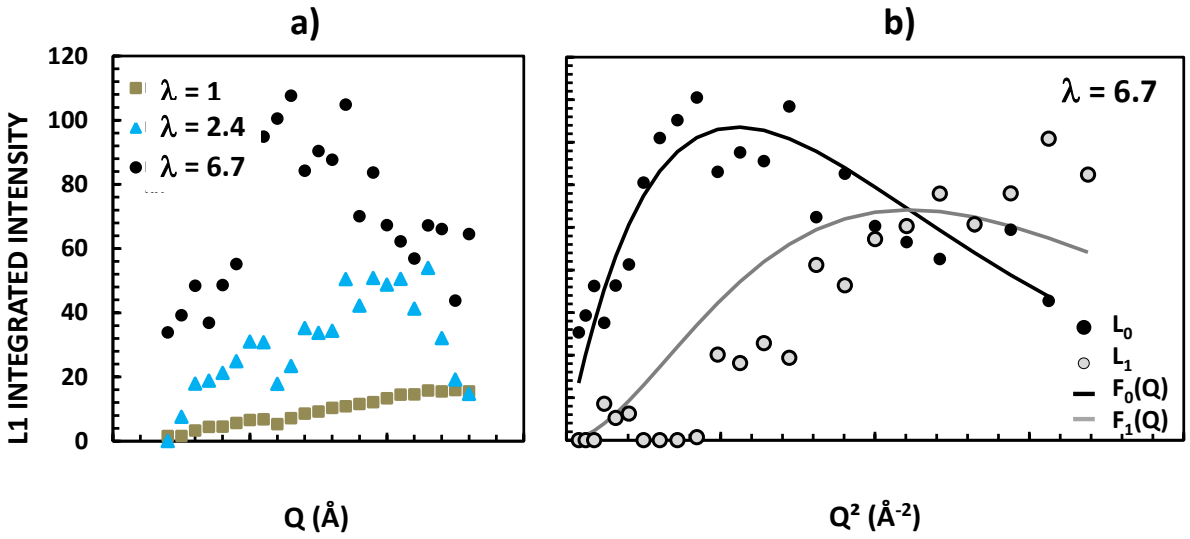

Figure SI 7. a) Integrated intensities of Lorentzian L_0 obtained after fitting the experimental S(Q,ω) of hybrid membranes at various hydrations using Eq. S8. **b)** Integrated intensities of Lorentzian L_0 and L_1 (dots) measured for the high hydration membrane, fitted with the Gaussian model structure factors (lines).

References for the SI:

S1 L. To Thi Kim, O. Sel, C. Debiemme−Chouvy, C. Gabrielli, C. Laberty-Robert, H. Perrot, C. Sanchez, *Electrochem. Comm.* **2010**, *12*, 1136.

S2 S. Tsushima, K. Teranishi, S. Hirai, *Energy* **2005**, *30*, 235.

S3 C. Wakai, T. Shimoaka and T. Hasegawa, *Analytical Chemistry* **2013**, *85*, 7581.

S4 F. Volino, J.C. Perrin, S. Lyonnard, *J. Phys. Chem. B*, **2006**, *110*, 11217.